

# Large Signal Modeling of AlGaN/GaN HEMTs with $P_{\text{sat}} > 4 \text{ W/mm}$ at 30 GHz suitable for Broadband Power Applications

F. van Raay, R. Quay, R. Kiefer, M. Schlechtweg, and G. Weimann

Fraunhofer Institute of Applied Solid-State Physics (IAF), Tullastr. 72, D-79108 Freiburg, Germany

**Abstract** — Large signal modeling and investigations of an AlGaN/GaN HEMT process on SiC with  $l_g = 150 \text{ nm}$  are performed with respect to broadband amplifiers up to 30 GHz. Output power values of 3.4 W or 4.25 W/mm at 18 GHz and  $P_{\text{out}} = 1.6 \text{ W}$  equivalent to 4 W/mm at 30 GHz are measured. The device modeling shows good agreement of the measured and modeled power sweeps at 10 GHz and 30 GHz. The large signal simulations show the suitability of AlGaN/GaN HEMTs for multi-band amplifiers in the K-band.

## I. INTRODUCTION

AlGaN/GaN HEMTs on SiC are being developed for high power applications due to their outstanding material properties combining both high breakdown fields and high saturation velocities. Developments so far mainly concentrated on the L-band (2 GHz) and X-band (8.2-12.4 GHz). Recently, reports on Ka-band operation were given in [1-3]. The contributions show that AlGaN/GaN HEMTs on SiC are very promising candidates for K- (18-26.5 GHz) and Ka-band (26.5-40 GHz) operation. This paper addresses thorough investigations and large signal modeling of AlGaN/GaN HEMT devices with respect to broadband power amplifiers. The output matching characteristics as a function of frequency are reported up to 30 GHz in agreement with active load-pull data which suggest very promising properties for high power broadband or multi-band amplifiers relative to e.g. GaAs PHEMT.

## II. SMALL-SIGNAL AND LARGE SIGNAL MEASUREMENTS

The devices under investigation have gate widths  $W_g$  of 0.1 mm to 0.8 mm, and a gate length of 150 nm. DC transconductance amounts to  $G_m > 250 \text{ mS/mm}$ , cut off frequencies  $f_T > 45 \text{ GHz}$  for a 0.4 mm device. A more thorough description of the technology is given in [2,3]. A scaled version of this process allowed for 40 GHz operation [3].

The large-signal measurement system is based on a Microwave Transition Analyzer HP 70820. Active load-pull using traveling wave tube amplifiers (with 10 W output power at 40 GHz) is performed according to [4]

with a system bandwidth of 50 GHz. This yields up to 5 harmonics in a 10 GHz measurement.

Fig. 1 shows a measured output power sweep at 18 GHz for a  $W_g = 0.8 \text{ mm}$  AlGaN/GaN device on SiC. A saturated output power of 35.3 dBm, a linear gain of 7.5 dB, and a maximum power added efficiency (PAE) of 18.1 % are measured at a  $V_{DS}$  bias of 30 V.

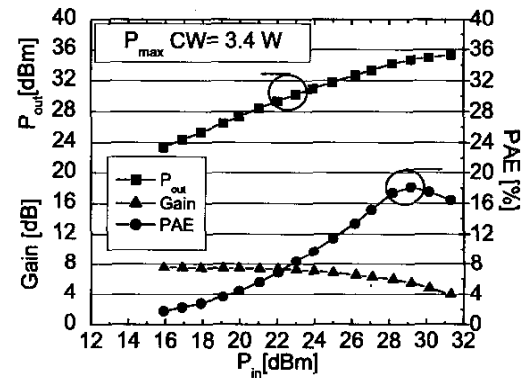


Fig. 1. Measured output power, gain, and power added efficiency vs. input power at 18 GHz for a  $W_g = 0.8 \text{ mm}$  device.

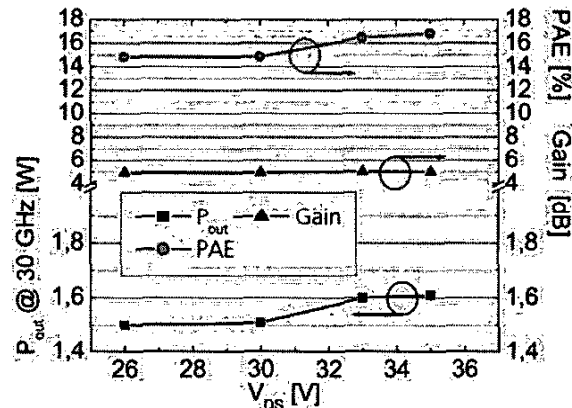


Fig. 2. Measured output power vs.  $V_{DS}$  voltage at 30 GHz for a  $W_g = 8 \times 50 \mu\text{m}$  device.

Fig. 2 shows the measured output power vs.  $V_{DS}$  voltage at 30 GHz. A maximum output power of 1.61 W equivalent to 4 W/mm is found at  $V_{DS} = 35$  V with a linear gain of 5 dB. Both Fig. 1 and 2 show the suitability of these devices for the K-band.

### III. LARGE SIGNAL MODELING

The principal strategy is to adopt sophisticated III-V HEMT modeling concepts to the AlGaN/GaN devices on SiC. Fig. 3 displays the used large signal model topology, which is similar to the one described in [5] for GaAs PHEMTs.

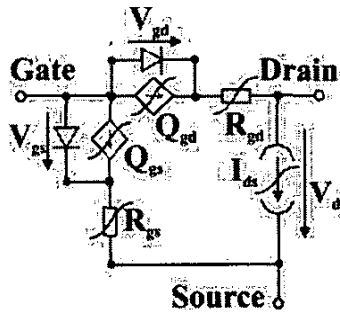


Fig. 3. Intrinsic part of Large Signal GaN HEMT Model.

In the first main step of the modeling approach, the bias-dependent elements of the corresponding small-signal circuit are extracted from 50 GHz S-parameters for approx. 400 bias points. Fig. 4 shows the extracted  $G_m$  and  $C_{gs}$  as a function of internal control voltages which are  $V_{gs}$  and  $V_{ds}$  for  $G_m$  and  $V_{gs}$  and  $V_{gd}$  for  $C_{gs}$ , respectively. Both 3D diagrams show the  $G_m$  and  $C_{gs}$  peaking vs. the junction voltage  $V_{gs}$ , which is typical for GaN HEMT devices. In contrast to GaAs HEMTs,  $G_m$  and  $C_{gs}$  are nearly independent of  $V_{ds}$  in the saturation region, i.e. there is only a slight decrease in the transit frequency for high  $V_{ds}$  values up to 40 V. This is of primary importance for fast high-power operation of the AlGaN/GaN devices.

For proper modeling of the gate-diode behavior of the AlGaN/GaN HEMTs, we found that a  $V_{ds}$  dependency of the barrier height  $\phi_b$  of the gate-source diode using two fitting parameters  $\alpha_b$  and  $\lambda_b$  had to be introduced which reads  $\phi_b(V_{ds}) = \phi_b(V_{ds}=0) - \lambda_b \tanh(\alpha_b V_{ds})$ .

In the second main modeling step the large-signal channel current  $I_{ds}(\text{RF})$  and charge sources  $Q_{gs}$  and  $Q_{gd}$  are calculated from the small-signal quantities by two-dimensional integration [5]. We use a combined approach for low-frequency dispersion and thermal modeling which is a simplified version of the method used in [5]. We extract the isothermal DC channel current and the RF

channel current from S-parameter measurements at room temperature (RT) and DC I-V-measurements at different temperatures only. Additionally, S-parameter measurements at temperatures between RT and 100 °C verify the combined dispersion and thermal modeling approach. Furthermore, DC pulse measurements at elevated temperatures using pulse widths down to 200 ns confirmed a DC to RF dispersion in  $G_m$  of less than 15%, which is similar to conventional GaAs PHEMT technologies. This weak dispersion is based on a careful optimization of the SiN passivation.

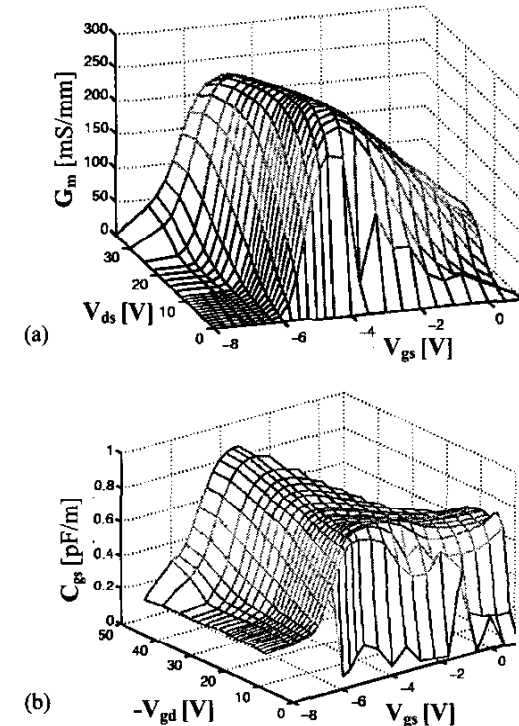


Fig. 4. Modeled  $G_m$  (a) and  $C_{gs}$  (b) as a function of internal control voltages.

Finally, the 2D-dependencies of these large-signal quantities are either fitted to analytical expressions or transformed into 2D-tables to end up either with an analytical or a table-based model, respectively. In this case we use an analytical model, and the  $I_{ds}$  current functions after Angelov et al. [6] had to be significantly modified with third-order polynomials in  $V_{ds}$  to fit the AlGaN/GaN HEMT behavior using the formula set

$$\begin{aligned}
 V_p &= V_{p0} - \delta V_{ds} \\
 \psi_1 &= P_{11} (V_{gs} - V_p) + P_{21} (V_{gs} - V_p)^2 + P_{31} (V_{gs} - V_p)^3 \\
 \psi_2 &= P_{12} (V_{gs} - V_p) + P_{22} (V_{gs} - V_p)^2 + P_{32} (V_{gs} - V_p)^3 \\
 \psi_3 &= \alpha_3 (V_{ds} - V_{gs} - V_{ds0}) + \beta_3 (V_{ds} - V_{gs} - V_{ds0})^2 + \gamma_3 (V_{ds} - V_{gs} - V_{ds0})^3
 \end{aligned}$$

$$I_{ds,DC}(V_{gs}, V_{ds}) = I_{pk} (1 + \tanh(\psi_1)) (1 + \lambda V_{ds}/(1 + (1 + \tanh(\psi_2) \psi_3)) \tanh(\alpha V_{ds})$$

where  $I_{pk}$ ,  $V_{p0}$ ,  $V_{ds0}$ ,  $\delta$ ,  $\alpha_3$ ,  $\beta_3$ ,  $\gamma_3$  and the  $P_{ik}$  values are formal fitting constants.

#### IV. MODEL VERIFICATION

A direct model verification of this modeling approach is performed at the device level for a GaN HEMT by means of large-signal waveform and load-pull measurements [4] instead of the widely used indirect verification using circuit designs. Fig. 5 shows the simulated and measured power sweep data at 10 GHz sinewave excitation at the gate for a device with  $2 \times 50 \mu\text{m}$  gate geometry. Magnitude and phase of the output wave at the drain are displayed. The measurement agrees well with the simulation within approx. 1 dB and 2.5 degrees of phase for the whole input power range.

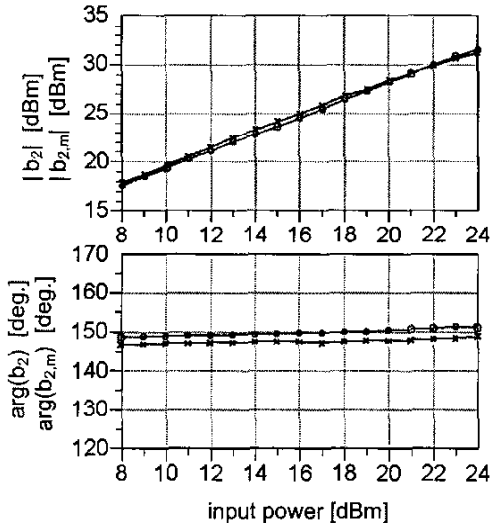


Fig. 5. Measured and simulated power sweep at 10 GHz for a  $2 \times 50 \mu\text{m}$  device. Crosses (blue): measurement, circles (red): simulation.

The waveform load-pull measurement allows a direct comparison of the measured and simulated dynamic load trajectories  $I_{DS}(V_{DS}(t))$  at the device level which are presented in fig. 6 for different RF input power levels. At 10 GHz the load reflection coefficient at the fundamental wave was tuned to maximum output power in this example. At a drain bias voltage of  $V_{DS} = 25 \text{ V}$ , a saturated output power density of  $5 \text{ W/mm}$  was achieved at 10 GHz. In fig. 6, a good agreement between the measured (bottom) and simulated (top) load trajectories is demonstrated.

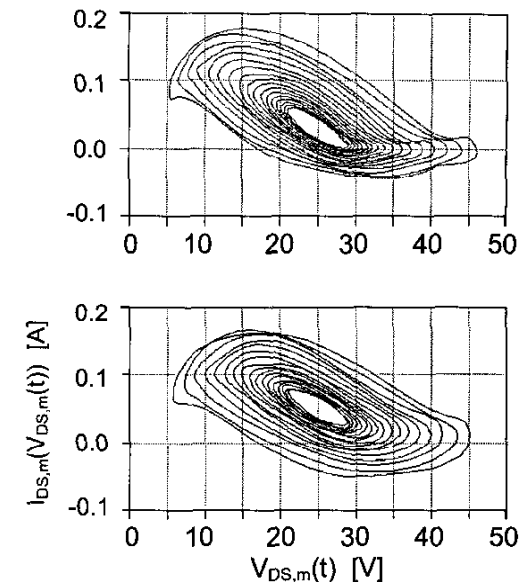


Fig. 6. Measured and simulated load trajectories at 10 GHz for a  $2 \times 50 \mu\text{m}$  device. Top (red): simulation, bottom (blue): measurement.  $P_{in} = 10 (1) 24 \text{ dBm}$ .

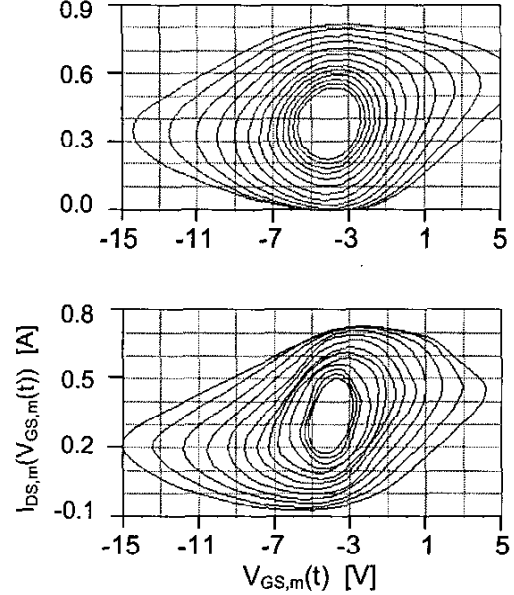


Fig. 7. Measured and simulated transfer trajectories at 10 GHz for an  $8 \times 100 \mu\text{m}$  device. Top (red): simulation, bottom (blue): measurement.  $P_{in} = 20 (1) 32 \text{ dBm}$ .

For simulation of large devices, a model for an  $8 \times 100 \mu\text{m}$  cell was extracted. Fig. 7 displays the time-domain transfer trajectories  $I_{DS}(V_{GS}(t))$  for different input power levels. Even for this large device, the agreement between

measurement and simulation is very good. In the entire power sweep, the deviation between measured and simulated output wave  $b_2$  was less than 1 dB.

Fig. 8 presents a power sweep of the output power wave at the drain of the device vs. the input power wave at the gate at 30 GHz. Here, the higher harmonics are not accessible due to the bandwidth limit of the measurement system. In this example, the device has a  $8 \times 50 \mu\text{m}$  gate geometry. For the simulation, the model for the  $8 \times 100 \mu\text{m}$  cell was scaled down to  $8 \times 50 \mu\text{m}$ . Here, the magnitude deviation between measurement and simulation is around 1 dB, while the phase difference is approx. 12 degrees. This demonstrates the scalability of the device model, especially for frequencies up to 30 GHz.

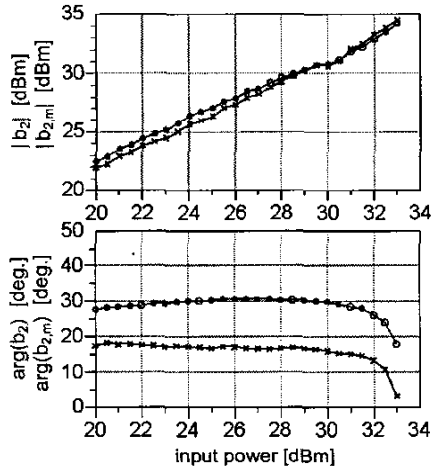


Fig. 8 Measured and simulated power sweep at 30 GHz for a  $8 \times 50 \mu\text{m}$  device. Crosses (blue): Measurement. Circles (red): Simulation.

## V. ALGAN/GAN HEMTs FOR BROADBAND AMPLIFIERS

With the verified model, predictions usable for MMIC design can be made. Fig. 9 shows the simulated and measured optimum output match between 18 GHz and 30 GHz obtained by harmonic balance simulations. Compared to a typical GaAs PHEMT, model and measurement of the GaN HEMT imply a load impedance level of  $30 \Omega$ , which simplifies matching to  $50 \Omega$  environment, while the PHEMT yields a considerably lower load impedance value around  $7 \Omega$ . This makes AlGaN/GaN devices extremely suitable for high power broadband amplifiers at least up to 30 GHz.

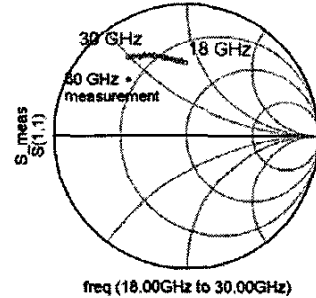


Fig. 9 Measured and simulated output load between 18 GHz and at 30 GHz for an  $8 \times 50 \mu\text{m}$  device.

## VI. CONCLUSION

Large signal investigations of a 150 nm AlGaN/GaN HEMT process have been performed. Output power values of  $P_{\text{out}} = 1.6 \text{ W}$  equivalent to  $4 \text{ W/mm}$  are measured at 30 GHz. Large signal modeling of the GaN HEMT devices is performed based upon a nonlinear circuit topology and a good agreement between measurement and simulation is demonstrated for waveform data at 10 GHz and power sweeps at 30 GHz.

## ACKNOWLEDGEMENT

The authors wish to acknowledge the continuing support of the German Federal Ministry of Education and Research (BMBF), and the German Federal Ministry of Defense (BMVg).

## REFERENCES

- [1] K. Kasahara, et al., "Ka-band 2.3W Power AlGaN/GaN Heterojunction FET", Int'l. Electron. Dev. Meeting 2002, San Francisco, December 2002, pp. 677 - 680.
- [2] R. Kiefer, et al., "AlGaN/GaN HEMTs for Power Applications up to 40 GHz", Proc. IEEE Lester Eastman Conf. High Perf. Dev. 2002, Newark, pp. 502-504.
- [3] R. Quay, et al., "AlGaN/GaN HEMTs on SiC Operating at 40 GHz", Int'l. Electron. Dev. Meeting 2002, San Francisco, pp. 673 - 676.
- [4] F. van Raay, G. Kompa, "A 40 GHz Large-Signal Double-Reflectometer Waveform Measurement System Designed for Load-Pull Applications", 26th European Microwave Conference, Prague, 1996, pp.657-661.
- [5] I. Schmale, G. Kompa, "A Symmetric Non-Quasi-Static Large-Signal FET Model with a Truly Consistent Analytic Determination from DC- and S-Parameter Data", 29th European Microwave Conference, Munich, October 1999, pp. 258 - 261.
- [6] I. Angelov, L. Bengtsson, M. Garcia, "Extensions of the Chalmers Nonlinear HEMT and MESFET Model", IEEE Trans. on MTT, vol. 44, no. 10, Oct. 1996, pp. 1664-1674.